Sjostrom, T., Nobbs, A., & Su, B. (2016). Bactericidal nanospike surfaces via thermal oxidation of Ti alloy substrates. Materials Letters, 167, 22-26. DOI: 10.1016/j.matlet.2015.12.140

Peer reviewed version

Bactericidal nanospike surfaces via thermal oxidation of Ti alloy substrates

Terje Sjöström, Angela H Nobbs and Bo Su*

School of Oral and Dental Sciences, University of Bristol, Lower Maudlin Street, BS1 2LY, UK

*corresponding author: b.su@bristol.ac.uk

Highlights

- Thermal oxidation was used to grow bioinspired nanospikes on Ti alloy.
- Nanospike dimension and arrangement could be controlled.
- The method worked on arbitrary shaped Ti alloy surfaces.
- A 40 % reduction of *E. Coli* viability was achieved on Ti alloy nanospike surfaces.

Abstract

With the aim to fabricate bio-inspired antibacterial nanotopography surfaces, nanospikes with varying dimensions were grown on Ti alloy surfaces using a thermal oxidation method. By controlling the acetone vapour concentration inside the tube furnace, the resulting oxide surface changed from nanocolumn shapes to nanospikes with approximately 20 nm diameters. The nanospikee growth was demonstrated to work on 3D Ti alloy bead surfaces, which means translation of the method to implant surfaces would be possible. Microbiology studies using *Escherichia coli*. showed that the nanospikes on the Ti alloy surfaces has potential to reduce bacterial viability. More dead bacteria were present on the nanospike surfaces compared to a smooth control and a 40 % reduction of viability was noted in bacterial suspensions incubated with a nanospike surface. It was shown that by annealing the Ti alloy surfaces prior to thermal oxidation, it is possible to grow vertically aligned nanospikes. This could be highly valuable when designing implant surfaces with antimicrobial properties.

Keywords: Biomaterials, Biomimetic, Metals and alloys, Oxidation

1. Introduction

Biofilm formation on surgical implants and the resulting infection is a major challenge in the biomaterials and medical devices field. Infection can result in traumatic and costly revision surgery [1-3], and the prevention of such infection, without impeding the function of the implant, is of high importance. Antimicrobial Ti and Ti alloy implant surfaces have been achieved with binding of antibiotics [4], antimicrobial peptides [3] or nanoparticles that have bactericidal effects [1], to the surface of the implant. A more favourable method of preventing Ti implant infection that could help combat the use of antimicrobials and thus the risk of driving development of antimicrobial resistance, is to use surface topography that actively discourages bacterial adhesion or has inherent antimicrobial properties, without the addition of antibiotics or other chemicals.

It is thought that nanostructures can cause damage to bacteria by piercing the cell membrane [5, 6]. Recently, Ivanova et al. [7-9] have demonstrated that nanopillar features on cicada wing surfaces have a bactericidal effect, which prevents biofilm formation by physically damaging bacterial cell walls. This effect was reproduced with similar topographies on both black silicon [8] and PMMA [10]. To achieve antimicrobial nanopillar surfaces on Ti and Ti alloy implants, a fabrication technique is needed that can mimic the dimensions of such surface features found in nature, ideally on arbitrary shaped and porous materials. To achieve nanostructures on Ti-6Al-4V (Ti64) surfaces with dimensions similar to those on the cicada wing, this study utilises a thermal oxidation technique that allows for tuning of the dimensions of the resulting nanospikes.

2. Materials and Methods

2.1 Thermal oxidation

Ti64 samples were placed in the centre of a horizontal alumina tube furnace (1500 mm long, 95 mm inner diameter). After purging the tube with Ar the temperature was increased to 850°C at 15°C/min. After reaching 850°C the Ar flow was diverted through a bubbler bottle containing acetone at 25°C with the Ar flow rate adjusted to a rate in the range of 50 – 300 sccm. The temperature was kept at

850°C for 45 minutes, after which the tube was allowed to cool under a flow of Ar at 500 sccm. To remove the carbon from the as-synthesized nanospikes, the samples heated to 600°C at a rate of 10°C/min. A JEOL JSM 5600LV scanning electron microscope (SEM) was used to image the oxidised Ti64 surfaces.

2.2 Bacterial growth conditions. E. coli (K12) was inoculated into Tryptic Soy Broth (TSB) (Oxoid) and grown at 37°C with agitation (220 rpm) for 16 h. Cultures were diluted to OD_{600} = 0.1 in fresh TSB and further incubated until mid-exponential phase was reached. Bacteria were then harvested (5000 *g*, 7 min) and the cell pellet was re-suspended in 5 ml TSB. This procedure was repeated twice and the cell suspension was then adjusted to OD_{600} = 0.3 for all experiments.

2.3 LIVE/DEAD staining. Aliquots (0.5 ml) of bacterial suspension were added to individual wells of a 24-well plate, each containing a 10 mm square Ti64 sample. Plates were then incubated for 2 h at 37°C in 5% CO_2. LIVE/DEAD Baclight L7007 component A (Invitrogen) was added to each well (3 µl/ml) and plates incubated in the dark for 15 min. Suspensions were then aspirated and the Ti64 samples gently rinsed with 10 mM Tris-HCl buffer at pH 7 (Sigma) to remove excess stain and non-adherent bacteria. Samples were then visualised by fluorescence microscopy (Leica DMLB).

2.4 Viability assay. Ti64 samples were incubated with bacteria as above for 2 h. Aliquots (90 µl) of bacterial suspension were transferred from each plate to individual wells of a 96-well microtitre plate and 10 µl PrestoBlue (Invitrogen) was added. Plates were incubated for an additional 30 min, and the fluorescence intensity of each well was then measured using a Tecan plate reader with excitation filter at 560 nm and emission filter at 590 nm.

3. Results and Discussion

3.1 Fabrication of nanospikes

The SEM images in Figure 1 shows the synthesized nanospikes after removal of the outer carbon shell. The as-synthesized nanospikes consist of a TiC core with a C shell [11], with the C shell removed and the TiC core converted to TiO_2 when heated in an atmospheric condition [12]. The nanospikes became thinner with increased acetone vapour in the tube furnace. By tuning the flow rate through the acetone bubbler, and thereby increasing the amount of acetone vapour in the tube furnace, the geometry of the nanospikes could be tuned from column-shaped structures to very thin wires with diameters in the region of 20 nm. With an increased carbon layer on top of the TiC, diffusion of Ti species from the substrate is reduced and therefore the growth of the inner TiC core is reduced [13], ultimately resulting in thinner spikes after removal of the carbon layer.

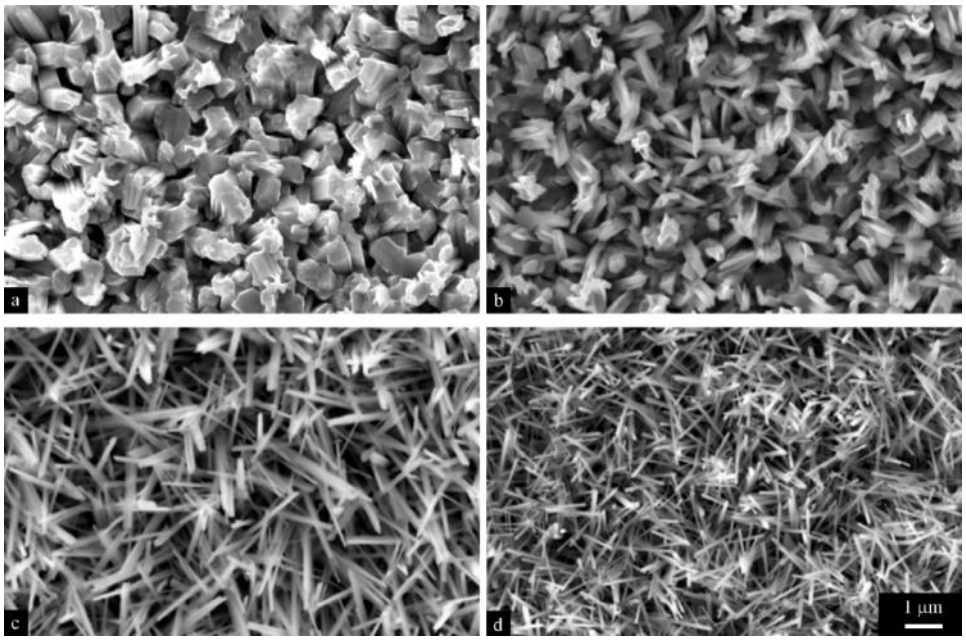

Figure 1

Apart from controlling the diameters of the TiO_2 nanospikes, we further attempted to grow vertically aligned nanospikes on the Ti64 substrates. After pre-annealing under vacuum at 1100°C the nanospikes were aligned in small bundles (Figure 2a). When the annealing temperature was increased to 1200°C the nanospike growth took place in an aligned manner, resulting in regions of perfectly vertical nanospikes from the substrate as shown in Figure 2b. It should be noted that whilst relatively

large areas displayed the aligned nanospikes (Figure 2c), other regions on the substrate displayed a more random arrangement of the nanospikes. Annealing of the Ti64 substrate prior to thermal oxidation influences the nanospike growth in several ways. Firstly, annealing of Ti64 promotes β-phase transformation, which can result in more prominent nanospike growth [14]. The fact that the nanospikes aligned, suggests that the annealing resulted in increased grain sizes with the nanospikes growing in an aligned manner when a certain crystal facet was exposed. It is known that the surface grain orientation can impact the arrangement of nanowires [15, 16] with TiO_2 nanowire growth taking place preferentially along the [110] direction in an oxygen deficient environment [17]. Because no attempt was made to expose a specific crystal facet, this could explain why nanospike alignment was only noticed on selected areas of the pre-annealed substrates.

To demonstrate the possibility to pattern three dimensional surfaces Ti64 beads were thermally oxidised. The resulting nanospikes on the beaded surfaces after processing with a 300 sccm flow rate are shown in Figure 2d. The nanospikes showed an excellent coverage on all parts of the beaded surfaces, demonstrating that the technique can be translated to more complex-shaped surfaces.

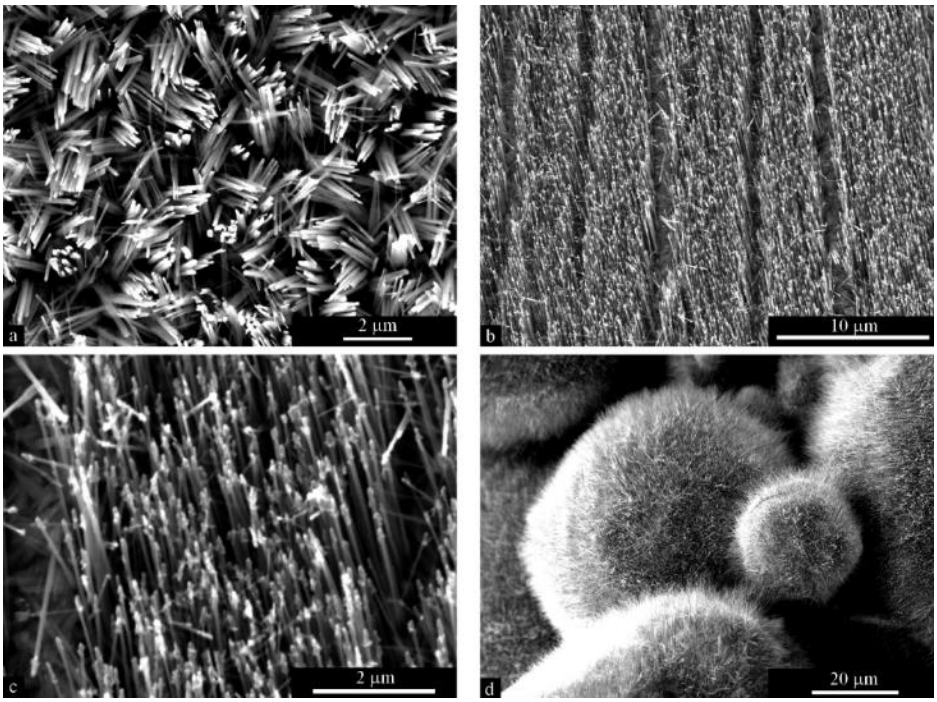

Figure 2

3.2 E. coli in vitro study

Suspensions of *E. coli* were incubated on both column-shaped features (50 sccm) and nanospikes (300 sccm). As-polished surfaces were used as control. LIVE/DEAD staining revealed more dead bacteria on the nanospike surface compared to the control (Figure 3a and b). The results were confirmed by resazurin-based PrestoBlue viability assay which measures viability of bacteria. Bacterial viability was reduced by approximately 40 % when incubated for 2 h with the nanopatterned surfaces as compared to the control surface (Figure 3c). Finally, the same PrestoBlue assay was conducted after the test surfaces had been coated with a 10 nm gold layer (Figure 3d). Even when gold-coated, nanospike surfaces resulted in a reduction in fluorescence and thus reduced bacterial viability relative to the control surface. This implied that the bactericidal effects were indeed caused by the topography of the surfaces and not the surface chemistry, in agreement with what has been found for both cicada wing surfaces [9] and black silicon surfaces [8].

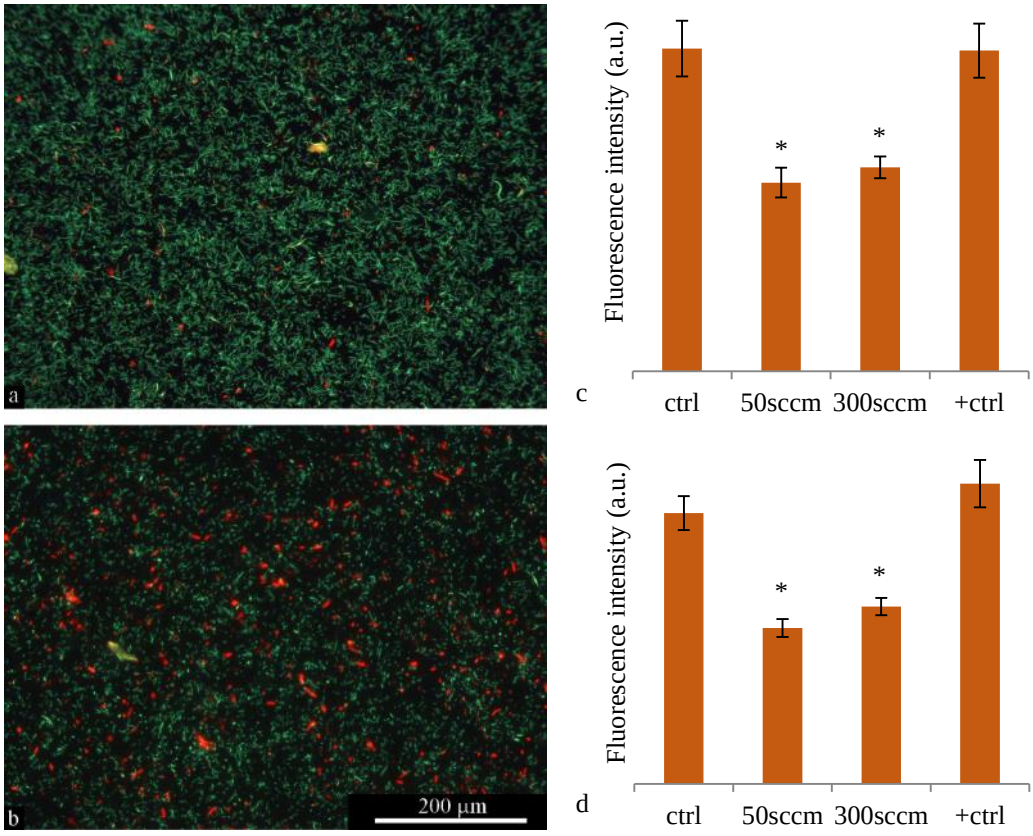

Figure 3

To achieve effective bacterial lysis, the bacteria need to be exposed to topographies that generate sufficient local stress across the bacterial cell wall. This requires contact points between the bacterial cell wall and the surface that are much smaller than the bacteria and with sufficient spacing in between the contact points. Dickson et al. [10] suggested that the spacing in between nanopillars should be between 130-380 nm. The nanospikes on our surfaces are more closely packed, but the random arrangement of the spikes means that bacteria can be exposed to sufficient local stress at selected points. The surfaces oxidised with the 50 sccm flow rate had diameters typically of 200-300 nm and were much shorter than the 300 sccm nanospikes. These columnar-shaped structures did however have sharp edges and pyramid shaped tips, features that was also noted during synthesis of TiC crystals [18], and which may be sufficient for physical damaging of the bacterial cell membrane. Gorth et al. [19] similarly noticed that the sharp edges on grains on a Si_3N_4 surface appeared to cause bacterial lysis, suggesting that a sharp nanopillar-type feature is not necessarily the only nanofeature that is capable of damaging bacterial cell walls.

4. Conclusions

Thermal oxidation of Ti64 surfaces was used to produce tuneable nanotopographies with the aim to fabricate implant surfaces that could physically deter bacterial colonisation. The nanospikes produced on the Ti64 surfaces in the current work had sharp tips or edges that mediate bactericidal effects upon *E. coli* , thereby reducing the chance of bacterial colonisation.

Acknowledgements

The work presented in this article was funded by the EPSRC, *Grant ref.* (EP/K035142/1). SEM studies were carried out in the Chemical Imaging Facility, University of Bristol with equipment funded by EPSRC under Grant *"Atoms to Applications", Grant ref.* (EP/K035746/1).

References

[1] Taylor E, Webster TJ, Reducing infections through nanotechnology and nanoparticles, International Journal of Nanomedicine 6 (2011) 1463-73.

[2] Darouiche RO, Current concepts - Treatment of infections associated with surgical implants, New England Journal of Medicine 350 (2004) 1422-9.

[3] Kazemzadeh-Narbat M, Kindrachuk J, Duan K, Jenssen H, Hancock REW, Wang RZ, Antimicrobial peptides on calcium phosphate-coated titanium for the prevention of implant-associated infections, Biomaterials 31 (2010) 9519-26.

[4] Hickok NJ, Shapiro IM, Immobilized antibiotics to prevent orthopaedic implant infections, Advanced Drug Delivery Reviews 64 (2012) 1165-76.

[5] Kang S, Herzberg M, Rodrigues DF, Elimelech M, Antibacterial effects of carbon nanotubes: Size does matter, Langmuir 24 (2008) 6409-13.

[6] Liu SB, Wei L, Hao L, Fang N, Chang MW, Xu R, et al., Sharper and Faster "Nano Darts" Kill More Bacteria: A Study of Antibacterial Activity of Individually Dispersed Pristine Single-Walled Carbon Nanotube, Acs Nano 3 (2009) 3891-902.

[7] Hasan J, Webb HK, Truong VK, Pogodin S, Baulin VA, Watson GS, et al., Selective bactericidal activity of nanopatterned superhydrophobic cicada Psaltoda claripennis wing surfaces, Applied Microbiology and Biotechnology 97 (2013) 9257-62.

[8] Ivanova EP, Hasan J, Webb HK, Gervinskas G, Juodkazis S, Truong VK, et al., Bactericidal activity of black silicon, Nature Communications 4 (2013) 7.

[9] Ivanova EP, Hasan J, Webb HK, Truong VK, Watson GS, Watson JA, et al., Natural Bactericidal Surfaces: Mechanical Rupture of Pseudomonas aeruginosa Cells by Cicada Wings, Small 8 (2012) 2489-94.

[10] Dickson MN, Liang EI, Rodriguez LA, Vollereaux N, Yee AF, Nanopatterned polymer surfaces with bactericidal properties, Biointerphases 10 (2015).

[11] Hu LS, Huo KF, Chen RS, Zhang XM, Fu JJ, Chu PK, Core-shell TiC/C quasi-aligned nanofiber arrays on biomedical Ti6Al4V for sensitive electrochemical biosensing, Chemical Communications 46 (2010) 6828-30.

[12] Shimada S, A thermoanalytical study of oxidation of TiC by simultaneous TGA-DTA-MS analysis, Journal of Materials Science 31 (1996) 673-7.

[13] Zhang XM, Huo KF, Wang HR, Gao BA, Fu JJ, Hung TF, et al., Controlled Fabrication of Core-Shell TiO2/C and TiC/C Nanofibers on Ti Foils and Their Field-Emission Properties, Acs Applied Materials & Interfaces 4 (2012) 1037-42.

[14] Lee H, Dregia S, Akbar S, Alhoshan M, Growth of 1-D TiO2 Nanowires on Ti and Ti Alloys by Oxidation, Journal of Nanomaterials (2010) 7.

[15] Faruque MK, Darkwa KM, Watson CY, Waterman JT, Kumar D, Synthesis, structure, and biocompatibility of pulsed laser-deposited TiN nanowires for implant applications, Journal of Biomedical Materials Research Part A 100A (2012) 1831-8.

[16] Faruque MK, M-Darkwa K, Xu Z, Kumar D, Fabrication, characterization, and mechanism of vertically aligned titanium nitride nanowires, Applied Surface Science 260 (2012) 36-41.

[17] Liu HZ, Y.; Li, R.; Cai, M.; Sun, X., A facile route to synthesize titanium oxide nanowires via water-assisted chemical vapor deposition, Journal of Nanoparticle Research 13 (2011) 385-91.

[18] Song MS, Huang B, Huo YQ, Zhang SG, Zhang MX, Hu QD, et al., Growth of TiC octahedron obtained by self-propagating reaction, Journal of Crystal Growth 311 (2009) 378-82.

[19] Gorth DJ, Puckett S, Ercan B, Webster TJ, Rahaman M, Bal BS, Decreased bacteria activity on Si3N4 surfaces compared with PEEK or titanium, International Journal of Nanomedicine 7 (2012) 4829-40.

Figure captions

Figure 1. SEM images of nanospikes on Ti64 substrates after thermal oxidation at various Ar flow rates through the acetone bubbler. a) 50 sccm, b) 100 sccm, c) 200 sccm and d) 300sccm. All surfaces were imaged after removal of carbon at 600°C.

Figure 2. SEM images of Ti64 surface thermally oxidised at 300 sccm Ar flow rate after removal of carbon at 600°C. Figures a) – c) show the effect of annealing the Ti64 prior to oxidation. The surfaces were annealed at a) 1100°C and b), c) 1200°C under an Ar atmosphere. The surface annealed at 1100°C had small bundles of nanospikes arranged in parallel but with varying directions across the surface, whereas the the surface annealed at 1200°C resulted in large areas of nanospikes aligned in the same direction. Figure d) shows nanospike growth on Ti64 beads.

Figure 3. Fluorescence micrographs showing live (green) and dead (red) *E. coli* on a) smooth control and b) 300 sccm nanospikes after 2 h incubation. c) shows viability of *E. coli* in the bacterial suspension after incubation with the test surfaces, as measured with the PrestoBlue assay, and d) shows viability of *E. coli* incubated for 2 h on nanospike surfaces which had been coated with 10 nm gold. The results showed the same trend as for c), indicating that bacterial viability was reduced on the test surfaces independently of surface chemistry. * indicates lower viability compared to ctrl (*P<0.05). The control surface was an as-polished Ti64 surface and +ctrl is the viability of bacteria incubated in a well without a Ti64 substrate.